Journal of Zhejiang University-SCIENCE B 2026 27(1):58-72
www.jzus.zju.edu.cn; www.springer.com/journal/11585
E-mail: jzus_b@zju.edu.cn

Research Article
https://doi.org/10.1631/jzus.B2400167

PICK1 modulates the proliferation and migration of gastric cancer cells by regulating TLR4

Kaiqiang LI[1,2*], Yimin YANG[3*], Yaling WANG[1*], Jing JIN[1], Qianni WANG[1], Lina PENG[1], Aibo XU[1], Xuling LUO[3], Wei YANG[4], Peng XU[5], Bingyu CHEN[1,2✉], Ke HAO[1,2✉], Zhen WANG[1,2✉]

[1]*Laboratory Medicine Center, Allergy Center, Department of Transfusion Medicine, Zhejiang Provincial People's Hospital (Affiliated People's Hospital), Hangzhou Medical College, Hangzhou 310014, China*
[2]*Key Laboratory of Biomarkers and In Vitro Diagnosis Translation of Zhejiang Province, Hangzhou 310063, China*
[3]*College of Pharmaceutical Sciences, Zhejiang University of Technology, Hangzhou 310014, China*
[4]*Department of Biophysics and Department of Neurosurgery, The First Affiliated Hospital, Zhejiang University School of Medicine, Hangzhou 310058, China*
[5]*The Third Affiliated Hospital of Zhejiang Chinese Medical University, Hangzhou 310005, China*

Abstract: Protein interacting with C kinase 1 (PICK1) interacts with a variety of membrane proteins and receptors involved in nervous system diseases and multiple cancers. However, the role of PICK1 in gastric cancer remains unclear. In the present work, we explored the expression and interactions of PICK1 with Toll-like receptor 4 (TLR4) in gastric cancer. Clinical data analysis showed that PICK1 expression decreases and is predictive of worse outcomes in patients with gastric cancer. High PICK1 levels attenuate the proliferation and migration of gastric cancer cells, which is dependent on the TLR4/myeloid differentiation primary response 88 (MyD88) signaling pathway. Furthermore, in vitro experiments demonstrated that PICK1 affects the trafficking and degradation of TLR4 and promotes TLR4 degradation via autophagy in gastric cancer cells. Molecular dynamics simulations highlighted the binding strength and stability of the TLR4-PICK1 complex. Our study provides new insights into the cellular and pathological functions of PICK1 in gastric cancer.

Key words: Protein interacting with C kinase 1 (PICK1); Gastric cancer; Toll-like receptor 4 (TLR4); Myeloid differentiation primary response 88 (MyD88) signaling pathway; Autophagy

1 Introduction

Gastric cancer, which occurs in the digestive tract, is the third leading cancer in the world in terms of mortality (Siegel et al., 2023). Therapeutic strategies have advanced significantly in the past few years, including chemotherapy, radiotherapy, immunotherapy, and surgical resection; however, invasion and metastasis are still frequent and lead to poor outcomes in many patients (Batista et al., 2013; Lee et al., 2013; Park and Chun, 2013; Stein et al., 2014). Therefore, it is necessary to investigate the mechanisms of gastric cancer, improve the diagnosis and prognosis of patients, and enhance prevention strategies.

Protein interacting with C kinase 1 (PICK1), a peripheral membrane protein comprising the PSD-95/Discs-large/Zona Occludens-1 (PDZ) and Bin/Amphiphysin/Rvs (BAR) domains, can bind to a variety of lipid molecules and membrane proteins (Inoue, 2007; Hanley, 2008), such as acid-sensing ion channels, α-amino-3-hydroxy-5-methyl-4-isoxazolepropionic acid receptors, and erythblastic leukemia viral oncogene homolog 2/human epidermal growth factor receptor 2 (ErbB2/HER2) (Xia et al., 1999; Jaulin-Bastard et al., 2001; Baron et al., 2002; Hanley and Henley, 2005; Lu and Ziff, 2005; Rocca et al., 2008). Abnormal expression of PICK1 in the brain has been shown

✉ Zhen WANG, wangzhen@hmc.edu.cn
Ke HAO, haoke@hmc.edu.cn
Bingyu CHEN, chenbingyu@hmc.edu.cn
* The three authors contributed equally to this work
Zhen WANG, https://orcid.org/0000-0002-8581-4649
Ke HAO, https://orcid.org/0000-0002-8013-9277
Bingyu CHEN, https://orcid.org/0009-0009-6162-1365

Received Mar. 25, 2024; Revision accepted Sept. 23, 2024; Crosschecked Nov. 12, 2025; Published online Nov. 29, 2025

to correlate with nervous system diseases, such as epilepsy, schizophrenia, and Parkinson's disease (Giros et al., 1996; Jones et al., 1998; Torres et al., 2001; Gainetdinov and Caron, 2003; Lorgen et al., 2017). Recent studies suggest the important role of PICK1 in cancer progression and metastasis. For instance, increased expression of PICK1 contributes to the growth and migratory potential of astrocytic tumor cells (Cockbill et al., 2015). PICK1 is overexpressed in breast cancer and correlates with lymph node infiltration, tumor grade, and the expression of HER2/neu protein, indicating that it may serve as a prognostic biomarker and therapeutic target in invasive breast cancer (Zhang et al., 2010). Our previous study showed that PICK1 is involved in epithelial–mesenchymal transformation (EMT) and inhibits the progression of gastric cancer (Zhou et al., 2021); however, the details of this effect remain to be discovered.

Toll-like receptor 4 (TLR4) is a transmembrane pattern recognition receptor with an important role in innate and adaptive immune responses (Pasare and Medzhitov, 2005). Recently, several studies have demonstrated the vital role of TLR4 in the initiation, metastasis, and progression of cancer (Chen et al., 2008; Rakoff-Nahoum and Medzhitov, 2009). TLR4 is overexpressed in various solid tumors and cancer cell lines, such as colorectal, cervical, and breast cancers (Wang et al., 2010; Chen et al., 2015; Zhang and Zhang, 2017). Yang et al. (2016) have shown that TLR4/nuclear factor-κB (NF-κB) signaling is associated with the survival of oral squamous cell carcinoma patients. Moreover, high expression levels of TLR4 are associated with gastric cancer progression (Meliț et al., 2019). TLR4, a membrane protein, may contribute to the underlying mechanism of PICK1's role in gastric cancer.

In the present study, we aimed to explore whether PICK1 protein is involved in the proliferation and migration of gastric cancer cells and whether it has an interaction with TLR4 in gastric cancer.

2 Materials and methods

2.1 Microarray data

The messenger RNA (mRNA) expression profiles and data were downloaded from the Gene Expression Omnibus database (https://www.ncbi.nlm.nih.gov/geo), with 300 gastric cancer samples from the GSE62254 dataset and 200 from the GSE15459 dataset. Among these, eight unavailable samples were excluded from the GSE15459 dataset, leaving a total of 492 gastric cancer samples for analysis (Zhou et al., 2021).

2.2 Clinical specimens

The clinical specimens were obtained from the Department of Gastroenterology, Zhejiang Provincial People's Hospital and Shanghai Outdo Biotech Co., Ltd. (https://www.superchip.com.cn).

2.3 Immunohistochemical analysis

Fifty-six human gastric samples derived from the HStmA180Su16 tissue microarray were used to detect PICK1 expression by immunohistochemical (IHC) analysis. Specific antibodies against PICK1 (1∶2000 (volume ratio), HuaBio, Hangzhou, China) were employed to determine the staining density. Scores were calculated based on the staining intensity and percentage of positive tumor cells in the whole tissues, which were evaluated according to the Fromowitz standard. All staining results were assessed at 200× magnification, and at least three fields from each core were counted.

2.4 Cell culture and treatment

The human gastric cancer cell lines AGS (adenocarcinoma gastric cells; RRID: CVCL_0139), BGC-823 (bleeding gastric cancer-823; RRID: CVCL_3360), SGC-7901 (stomach gastric carcinoma cells-7901; RRID: CVCL_0520), HEK293T (human embryonic kidney 293T; RRID: CVCL_0063), and GES-1 (gastric epithelial cells-1; RRID: CVCL_EQ22) were purchased from the Chinese Academy of Sciences Cell Bank (Shanghai, China). All cells were grown in Dulbecco's modified Eagle's medium (DMEM; HyClone, Shanghai, China) supplemented with 10% (volume fraction) fetal bovine serum (FBS; Gibco, USA) and penicillin (100 U/mL)-streptomycin (0.1 mg/mL) in a cell incubator at 37 ℃ with 5% CO_2. To construct stable PICK1-overexpressing (OV-PICK1) gastric cells, AGS cells were infected with OV-PICK1 or control lentivirus at a multiplicity of infection (MOI) of 5 according to the manufacturer's instructions. After 24 h of infection, the cells were incubated with puromycin (5 μg/mL) for 10 d to select stably expressing cells. Lipopolysaccharide (LPS) extracted from *Escherichia coli* serotype O55∶B5 (LPS O55∶B5) (Sigma-Aldrich,

Dorset, UK) was dispersed in phosphate-buffered saline (PBS) at 100 ng/mL. For the in vitro experiments, the cells were incubated with LPS for 2 h before further examination. The cells were incubated with FSC-231 (15 μmol/L; Merck, Shanghai, China), MG132 (1 μmol/L; Merck), and chloroquine (CQ) (30 μmol/L; Merck) for 24 h.

2.5 Cell growth and proliferation

The cell suspension was added to 96-well plates. After 24 h, the original culture medium in the well plate was replaced with 100 μL of cell counting kit-8 (CCK-8) solution (Vazyme, Nanjing, China) (culture medium:CCK-8 reagent=9:1 (volume ratio)). The cells were incubated for 2 h and the optical density (OD) value at 450 nm ($OD_{450\ nm}$) was measured by a microplate reader (Tecan, Männedorf, Switzerland).

The cell suspension was added to 6-well plates. After 10 d, the cells were washed with PBS. The cells were fixed with 4% (volume fraction) paraformaldehyde (Servicebio, Wuhan, China) for 15 min, then stained with crystal violet solution for 10 min and photographed.

2.6 Cell cycle fluorescence-activated cell sorting (FACS) analysis

The cell suspension was added to 12-well plates. After 24 h, serum-free medium was added for another 24 h to realize cell cycle synchronization. The treated cells were collected, fixed with pre-cooled 70% (volume fraction) ethanol, and then stained with propidium iodide (PI). The cell cycle was analyzed by flow cytometry (BD Biosciences, Franklin Lakes, NJ, USA).

2.7 Transwell migration assay

The treated AGS cell suspension was added to the upper chambers of 24-well plates (2×10^4 cells/well) with serum-free medium, while DMEM supplemented with 10% FBS was added to the lower chambers. After 24 h, the cells in the upper chambers were removed, and the cells passing through the membrane were fixed with 4% paraformaldehyde and stained with crystal violet solution. Images of cells were taken using a microscope (Nikon, Tokyo, Japan).

2.8 Scratch assay

The cell suspension was added to 6-well plates. Until the cells reached 90%–100% confluence, a 1-mm straight scratch on the wells was made using a sterile pipette tip, and 10 μg/mL mitomycin C (Sigma-Aldrich) was added for 1 h. The medium supplemented with low serum was added, and images of the scratches were captured at 0, 24, and 48 h. Images of cell migration were analyzed by ImageJ (National Institutes of Health, MD, USA), and wound healing ability was calculated and compared with the initial wound area.

2.9 Western blotting

Briefly, equal amounts (20–30 μg) of proteins were separated by sodium dodecyl sulfate-polyacrylamide gel electrophoresis (SDS-PAGE) and transferred onto polyvinylidene fluoride (PVDF) membrane (Millipore, Billerica, MA, USA). After blocking in 5% (0.05 g/mL) non-fat milk for 1 h, the membranes were incubated with primary antibodies overnight at 4 °C, including anti-cyclin-dependent kinase 4 (anti-CDK4) (1:1000 (volume ratio, the same below), HuaBio), anti-CDK6 (1:1000, HuaBio), anti-PICK1 (1:2000, HuaBio), anti-TLR4 (1:1000, HuaBio), anti-glyceraldehyde-3-phosphate dehydrogenase (anti-GAPDH) (1:5000, HuaBio), anti-myeloid differentiation primary response 88 (anti-MyD88) (1:1000, CST, Massachusetts, USA), anti-phospho-NF-κB (1:1000, CST), and interleukin-12 (IL-12) (1:1000, CST). The membranes were subsequently incubated with horseradish peroxidase (HRP)-labeled secondary antibodies (1:3000, HuaBio) for 2 h. The protein bands were detected by enhanced chemiluminescence (ECL) reagent (Beyotime, Shanghai, China) and the Bio-Rad imaging system (Bio-Rad, California, USA).

2.10 Immunofluorescence

Plasmids encoding PICK1 and TLR4 were purchased from Addgene (MA, USA). HEK293T cells were transfected with the PICK1 and TLR4 plasmids using Lipofectamine 3000 (Invitrogen, Carlsbad, CA, USA) for 72 h, followed by immunofluorescence staining. Briefly, HEK293T cells were fixed with 4% paraformaldehyde for 10 min and the cell membranes were permeabilized with 0.2% (volume fraction) Triton X-100 for 15 min. Then, the cells were blocked with 10% (0.1 g/mL) bovine serum albumin (BSA) and incubated with primary anti-PICK1 (1:500, NeuroMab, Davis, CA, USA) or anti-TLR4 (1:500, Abcam, Cambridge, UK) overnight at 4 °C, followed by incubation

with solution of secondary antibodies (Thermo Fisher Scientific, Rockford, IL, USA) for 1 h. 4',6-Diamidino-2-phenylindole (DAPI) was used for staining the cell nuclei. Finally, the fluorescent signals of cells were observed and captured using a confocal microscope (Leica SP8, Germany).

2.11 Co-immunoprecipitation

HEK293T cells were lysed in the immunoprecipitated radioimmunoprecipitation assay (IP-RIPA) buffer (Beyotime) and centrifuged at 16 000*g* at 4 ℃ for 12 min. The protein concentration was detected using a bicinchoninic acid (BCA) kit (Thermo Fisher Scientific). To detect the interaction between PICK1 and TLR4, the cell lysates were incubated overnight at 4 ℃ with negative control immunoglobulin G (IgG) (Invitrogen) or anti-PICK1 antibody, anti-TLR4 antibody, and protein A-Sepharose 4B beads (GE Healthcare, Pittsburgh, PA, USA). Proteins on the beads were collected using 2× SDS sample buffer, and finally boiled at 100 ℃ for 5 min prior to a western blotting test.

2.12 Surface plasmon resonance

Surface plasmon resonance (SPR) experiments were performed using a Biacore-8K (Cytiva, Massachusetts, USA). PICK1 proteins were immobilized on a CM5 chip (Cytiva) using the amino coupling method. TLR4 proteins were diluted from 100 to 50, 25, 12.5, 6.25, 3.12, and 1.56 nmol/L by 5% (volume fraction) dimethyl sulfoxide (DMSO) or PBS and injected into the flow cell at a flow rate of 30 μL/min. The contact time was 180 s and the dissociation time was 300 s. The results were analyzed using Biacore evaluation software (Wuhan, China).

2.13 Molecular dynamics simulations

Molecular dynamics (MD) simulations were conducted to evaluate the interactions between PICK1 and TLR4 at the atomic level. The three-dimensional (3D) structures of PICK1 and TLR4 were obtained using UniProt codes Q9NRD5 and O00206, respectively. They were optimized using Alphafold2 (Vani et al., 2024), followed by the University of California San Francisco (UCSF) chimeras to remove water molecules and unrelated heteroatoms (Bedart et al., 2022). All MD simulations were performed using Gromacs 5.1.5 (GNU General Public License, Groningen, the Netherlands). The temperature (298.15 K), pH (7), and pressure (1 bar per atmosphere (atm); 1 bar=100 kPa, 1 atm=101.325 kPa) were selected to build the all-atom model system with the AMBEff14SB position parameters (Bedart et al., 2022). TIP3P was used for the water molecular simulations (Mohammadi et al., 2023). After 1000 ps of energy minimization, the system was balanced within the nucleus ventralis tuberis (NVT) and nucleus posterior tuberis (NPT) procedures. We performed 50 ns MD simulations, with 2 fs per step. After all simulations were completed, the gmx module was used to calculate the radius of gyration (R_g), hydrophobic contact, and root-mean-square deviation (RMSD).

2.14 Binding energy analysis

The binding energies between PICK1 and TLR4 were calculated using molecular mechanics with generalized Born and surface area solvation (MM/GBSA) implemented in the MMPBSA package (Shoaib et al., 2023). In the MM/GBSA method, the binding-free energy (ΔG_{bind})=$\Delta H - T_{\Delta S} \approx \Delta G_{solv} + \Delta G_{gas} - T_{\Delta S}$, where gas-phase energy (ΔG_{gas}) denotes the kinetic energy in vacuum before and after the binding, including internal energy (E_{int}), van der Waals energy (E_{vdW}), and electrostatic energy (E_{elec}); solvation-free energy (ΔG_{solv}) is a solvent effect term, divided into the polar term polar solvation-free energy (ΔE_{GB}) and the nonpolar term nonpolar solvation-free energy (ΔE_{surf}); and $-T_{\Delta S}$ denotes the entropy change, which reflects the energy loss caused by the flexibility or stability of the system, which was ignored in accordance with several studies (Yan et al., 2020).

2.15 Statistical analysis

All data were presented as mean±standard deviation (SD). Statistical analyses were performed using unpaired Student's *t*-tests in GraphPad Prism 9.0. The log-rank test and Kaplan-Meier analysis were carried out to analyze the differences in survival rates. $P<0.05$ was considered indicative of statistical significance.

3 Results

3.1 Expression of PICK1 in gastric cancer

We first detected PICK1 expression in several human gastric cells (SGC-7901, AGS, and BGC-823). As shown in Fig. 1a, human gastric cancer cells exhibited lower PICK1 levels than normal gastric cells

(GES-1). Moreover, PICK1 was lowly expressed in human gastric tissues (Fig. 1b). The information of the gastric cancer tissue samples is displayed in Table S1. Furthermore, we analyzed clinical data from 492 tumor cases taken from the GSE62254 and GSE15459 datasets (Table S2). Patients were grouped according to the optimal cut-off (Youden index) of PICK1 determined in our previous study (Zhou et al., 2021). Kaplan-Meier survival analysis demonstrated that patients in the PICK1 low-expression group had a lower probability of survival than those in the high-expression group (Fig. 1c). The IHC data showed that PICK1 expression was significantly lower in gastric cancer tissue samples (Figs. 1d and 1e), and PICK1 expression was correlated with lymph node metastasis and higher clinical stage (Tables 1 and S3).

3.2 Effects of PICK1 overexpression on the growth and cell cycle of gastric cancer cells

We next examined the biological effects of PICK1 overexpression in gastric cancer cells. As shown in Figs. 2a and 2b, we overexpressed PICK1 in AGS cells and validated its efficiency using western blotting. Notably, PICK1 overexpression significantly suppressed gastric cell growth (Figs. 2c and 2d). Flow cytometry revealed that the arrest of AGS cells at the

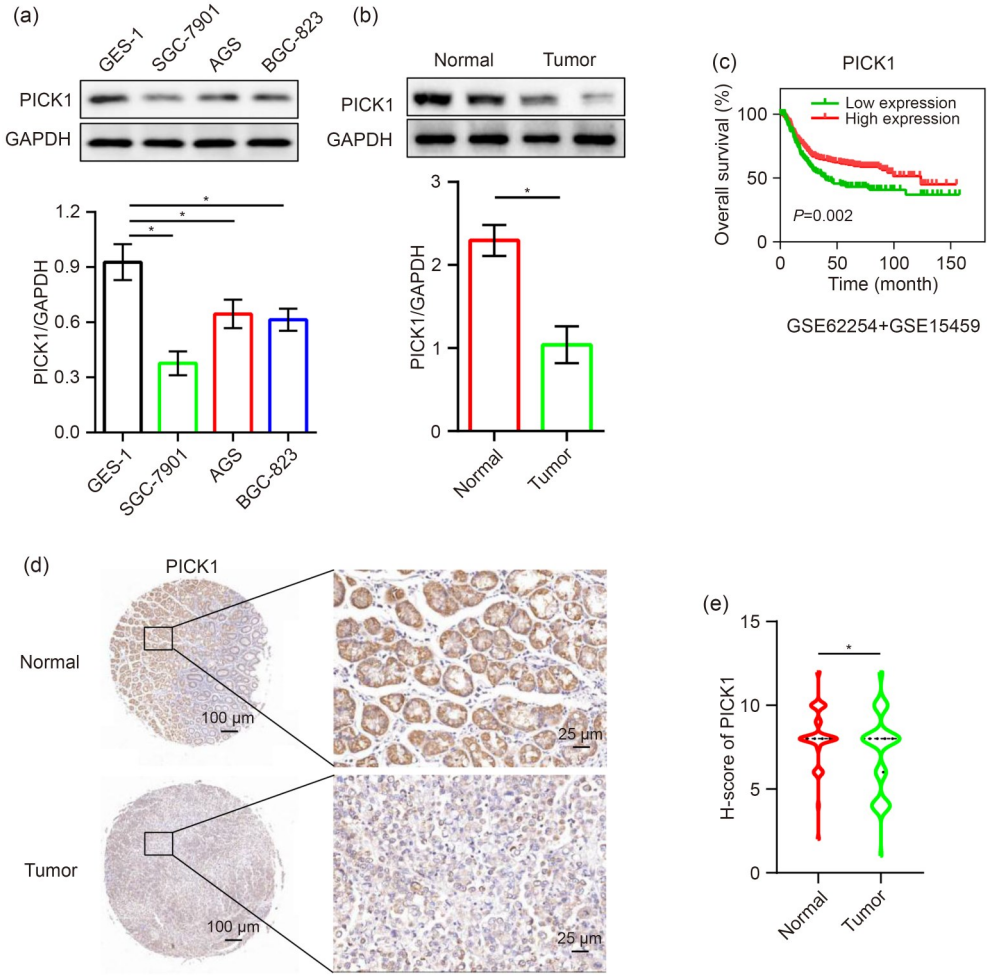

Fig. 1 Expression and Kaplan-Meier survival analysis of PICK1. (a) Western blot showing the expression of PICK1 in human normal gastric cells (GES-1) and gastric cancer cells (SGC-7901, AGS, and BGC-823). (b) PICK1 expression in gastric tissues. (c) Kaplan-Meier survival analysis of high and low expression of PICK1 in gastric tissues using the GSE62254 and GSE15459 datasets. (d, e) Immunohistochemical (IHC) analysis showing the expression of PICK1 in gastric tissue samples. (a, b) The data are represented as mean±SD, $n \geqslant 3$. $^{*}P<0.05$. SD: standard deviation; GES-1: gastric epithelial cells-1; SGC-7901: stomach gastric carcinoma cells-7901; AGS: adenocarcinoma gastric cells; BGC-823: bleeding gastric cancer-823; PICK1: protein interacting with C kinase 1; GAPDH: glyceraldehyde-3-phosphate dehydrogenase.

Table 1 Correlations between the PICK1 expression level in gastric tumor samples and clinical pathological characteristics of the corresponding patients

Characteristics	PICK1-low	PICK1-high	*P* value
Number	30	26	
Gender, *n* (%)			0.678
Male	18 (32.1)	17 (30.4)	
Female	12 (21.4)	9 (16.1)	
Age (years), *n* (%)			0.560
>60	21 (37.5)	20 (35.7)	
≤60	9 (16.1)	6 (10.7)	
Tumor invasion, *n* (%)			0.055
T1+T2	1 (2.0)	6 (11.8)	
T3+T4	27 (52.9)	17 (33.3)	
Lymph node metastasis, *n* (%)			0.019*
N0+N1	8 (14.3)	15 (26.8)	
N2+N3	22 (39.3)	11 (19.6)	
Distant metastasis, *n* (%)			1.000
M0	27 (48.2)	23 (41.1)	
M1	3 (5.4)	3 (5.4)	
Clinical stage, *n* (%)			0.003*
I+II	10 (17.9)	19 (33.9)	
III+IV	20 (35.7)	7 (12.5)	

PICK1: protein interacting with C kinase 1. * Low expression of PICK1 in gastric cancer tissues of patients was correlated with lymph node metastasis and tumor malignant progression.

G_0/G_1 phase was significantly promoted by PICK1 (Figs. 2e and S1). Western blotting analysis revealed that the expression of CDK4 and CDK6 was inhibited by overexpressed PICK1 (Fig. 2f).

3.3 Effects of PICK1 overexpression on migration and TLR4 protein expression of gastric cancer cells

Next, to investigate the effects of PICK1 overexpression on cell migration, we performed transwell and scratch assays. The results indicated that PICK1 overexpression significantly reduced the migratory ability compared to the control group (Figs. 3a and 3b). To determine the mechanisms of functional changes in gastric cells, we used western blotting to detect chronic inflammation in gastric cells. As shown in Figs. 3c and 3d, we found that the IL-12 protein expression level was lower in the PICK1 group. The TLR4/MyD88 signaling pathway is closely associated with chronic inflammation. The TLR4, MyD88, and phospho-NF-κB protein levels were significantly reduced by PICK1 overexpressed in AGS cells (Figs. 3c and 3d). Furthermore, we constructed the PICK1 PDZ-truncated plasmid, PICK mutant (Mut) (Fig. S2), and found that the PICK1 PDZ mutation had no significant effect on AGS cell proliferation, cell cycle, or TLR4 protein expression (Fig. S3). These results indicate that PICK1 plays an inhibitory role in the metastasis and inflammation of gastric cancer cells.

3.4 Effects of *PICK1* downregulation on proliferation and TLR4 protein expression in gastric cancer cells

Furthermore, we customized *PICK1* small interfering RNA (siRNA) for the downregulation of *PICK1* gene expression in AGS cells. The siRNA information is shown in Table S4, whereas Fig. 4a demonstrates the efficiency of *PICK1* knockdown in AGS cells infected with siRNA for 24 h. The CCK-8 results indicated that AGS cell proliferation was enhanced after *PICK1* gene downregulation (Fig. 4b). In addition, the flow cytometry results showed that the proportion of AGS cells blocked in the G_0/G_1 phase was reduced in the SA, SB, and SC groups (three types of *PICK1* siRNA) with a knockdown of *PICK1* compared with the control group (Fig. 4c). The protein expression levels of TLR4 and PICK1 were also examined. No significant changes in TLR4 protein levels occurred after knockdown of *PICK1* expression, which may be due to the low expression of PICK1 protein in AGS

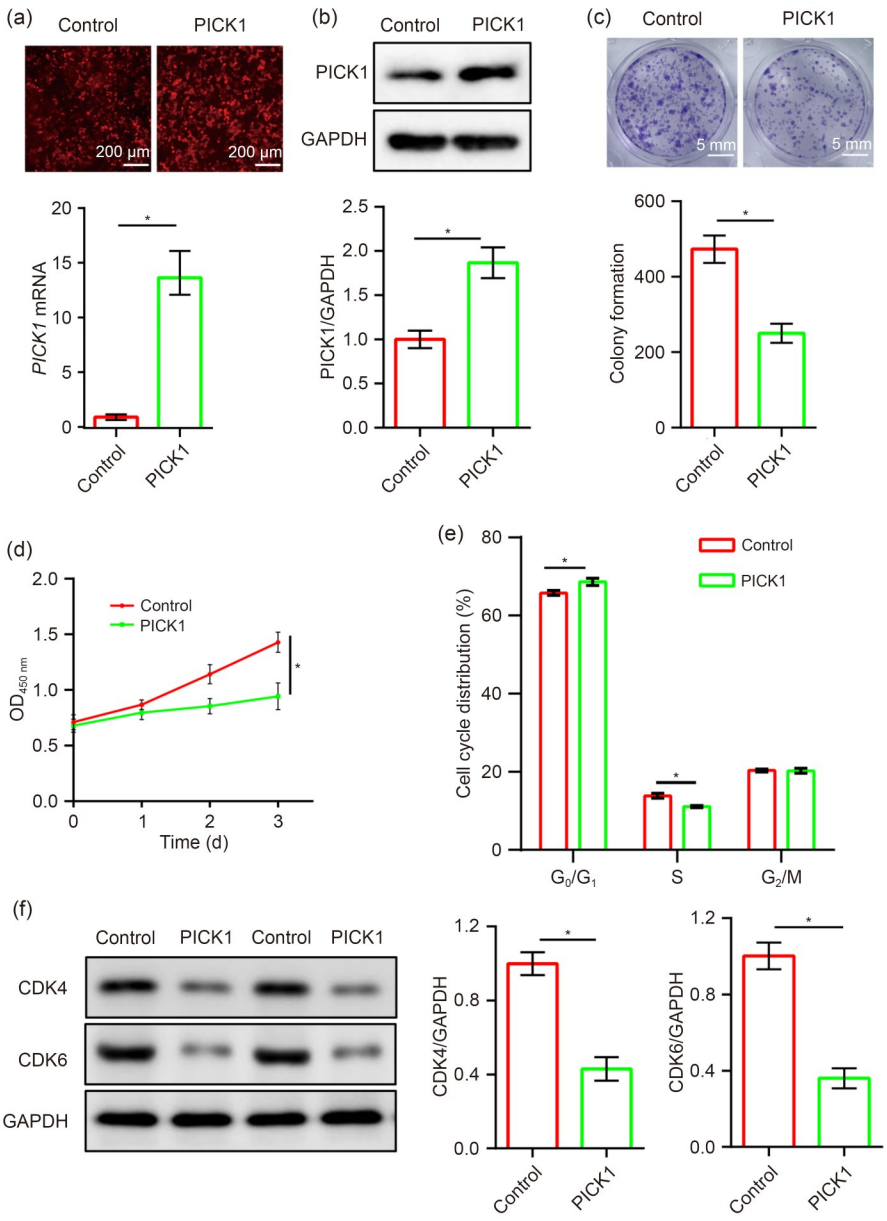

Fig. 2 Effects of PICK1 overexpression on AGS cell growth and cell cycle arrest. (a) After cells were infected with PICK1 or control lentivirus, the fluorescence intensity was observed using confocal microscopy (Leica SP8, Germany). (b) Efficiency was validated using western blotting. (c) Cell colony formation. (d) Results of the CCK-8 assay show the viability of stable PICK1-overexpressing or control cells. (e) Results of cycle analysis using flow cytometry. (f) Western blot showing the expression of CDK4 and CDK6 in each group. The data are presented as mean±SD, $n \geq 3$. $^{*}P<0.05$. SD: standard deviation; PICK1: protein interacting with C kinase 1; mRNA: messenger RNA; GAPDH: glyceraldehyde-3-phosphate dehydrogenase; $OD_{450\ nm}$: optical density at 450 nm; CDK4: cyclin-dependent kinase 4; CDK6: cyclin-dependent kinase 6; CCK-8: cell counting kit-8.

cells, resulting in the failure of knockdown to significantly affect TLR4 protein expression (Fig. 4d).

3.5 Interaction between PICK1 and TLR4

The 3D structure of PICK1 bound to TLR4 is illustrated in Fig. 5a. It can be found that the folded area of PICK1 is combined with a semi-circular groove in TLR4, forming hydrogen bonds, pi-stacks, and salt bridges (Fig. S4). PICK1 could bind with TLR4; the confidence of Rank1 was greater than 0.9, and the docking fraction was −261.85 kcal/mol (Table S5). The immunoprecipitation results revealed the interaction

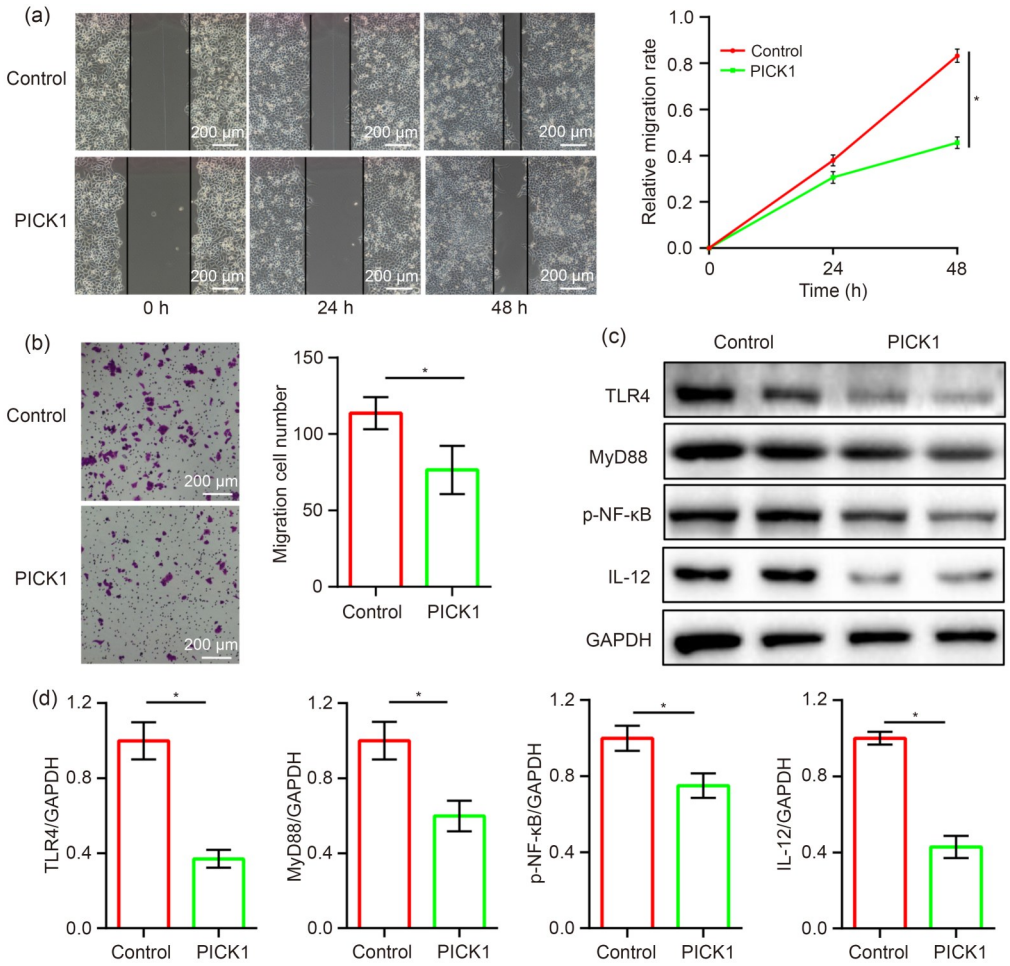

Fig. 3 Effects of PICK1 overexpression on cell migration and TLR4 protein expression in gastric cells. (a) Representative images of wound healing assays in AGS cells infected with the PICK1 or control lentivirus at 0, 24, and 48 h. (b) Transwell migration assay for the migratory capacity of AGS cells. (c, d) Relative protein levels of TLR4, MyD88, p-NF-κB, and IL-12 in AGS cells. The loading mode in the figure included two multiple holes. The data are presented as mean±SD, $n\geqslant 3$. * $P<0.05$. SD: standard deviation; PICK1: protein interacting with C kinase 1; GAPDH: glyceraldehyde-3-phosphate dehydrogenase; TLR4: Toll-like receptor 4; MyD88: myeloid differentiation primary response 88; p-NF-κB: phospho-nuclear factor-κB; IL-12: interleukin-12.

between PICK1 and TLR4 (Fig. 5b). Immunofluorescence using confocal microscopy (Fig. 5c) showed that PICK1 and TLR4 were both expressed in HEK293T cells and displayed a diffuse pattern in the cytoplasm. SPR assay was performed to detect the direct interaction between PICK1 and TLR4 (Fig. 5d), and the dissociation equilibrium constant (K_D) was 4.07 μmol/L. Furthermore, to investigate how PICK1 regulates TLR4 expression, PICK1-overexpressing AGS cells were treated with FSC-231 to suppress the PICK1 PDZ domain. As shown in Fig. 5e, FSC-231 treatment increased TLR4 expression. Moreover, when cells were treated with the autophagy activator MG132 and the autophagy inhibitor CQ, TLR4 expression was increased by CQ treatment (Fig. 5f). These results demonstrate that PICK1 binds to TLR4 and promotes TLR4 degradation by autophagy in gastric cells.

3.6 Binding energy of PICK1 and TLR4

We further calculated the binding energy of PICK1 to TLR4 using MD simulations (Table 2). The structural characteristics of the complex in the 50 ns MD simulations are shown in Fig. 6a. It can be found that the number of hydrogen bonds increased most obviously from the original 2 to 22, and the number of salt bridges increased from 2 to 6 at the end of the MD simulations (Figs. 6b–6d). The RMSD and R_g values indicated that the protein-binding mode was stable

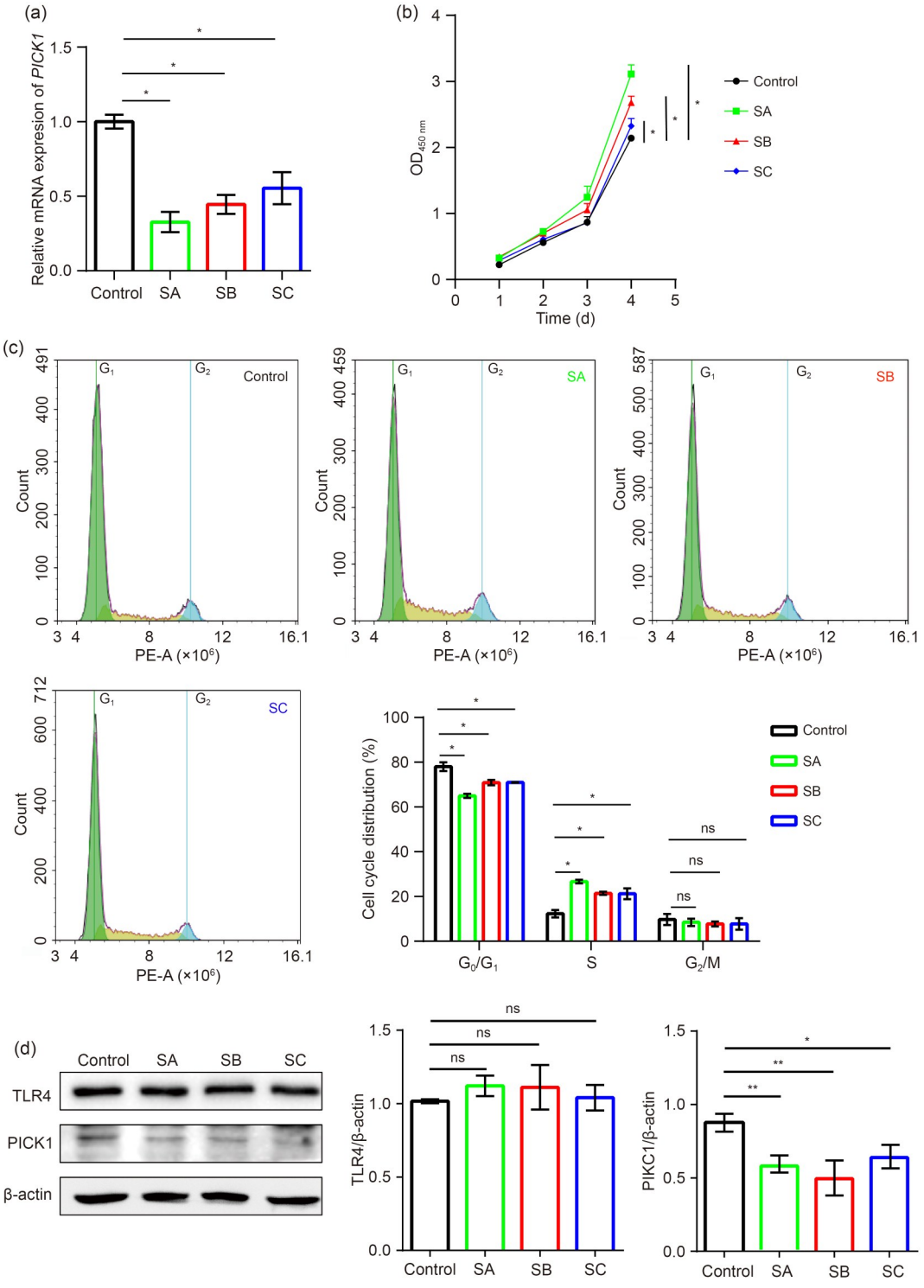

Fig. 4 Effects of downregulation of *PICK1* gene in AGS cells. (a) *PICK1* gene expression in AGS cells infected with SA, SB, and SC siRNAs for 24 h. (b) Growth curves of AGS cells infected with SA, SB, and SC siRNAs for 48 h. (c) Cell cycle of AGS cells infected with SA, SB, and SC siRNAs for 48 h. (d) TLR4 and PICK1 protein expression in AGS cells infected with SA, SB, and SC siRNAs for 48 h. The data are presented as mean±SD, $n \geqslant 3$. $^{*}P<0.05$; $^{**}P<0.01$; ns: no significant difference. SD: standard deviation; $OD_{450\ nm}$: optical density at 450 nm; PICK1: protein interacting with C kinase 1; TLR4: Toll-like receptor 4; GAPDH: glyceraldehyde-3-phosphate dehydrogenase; SA, SB, SC: *PICK1* small interfering RNA (siRNA) (three types); mRNA: messenger RNA; PE-A: phycoerythrin-area.

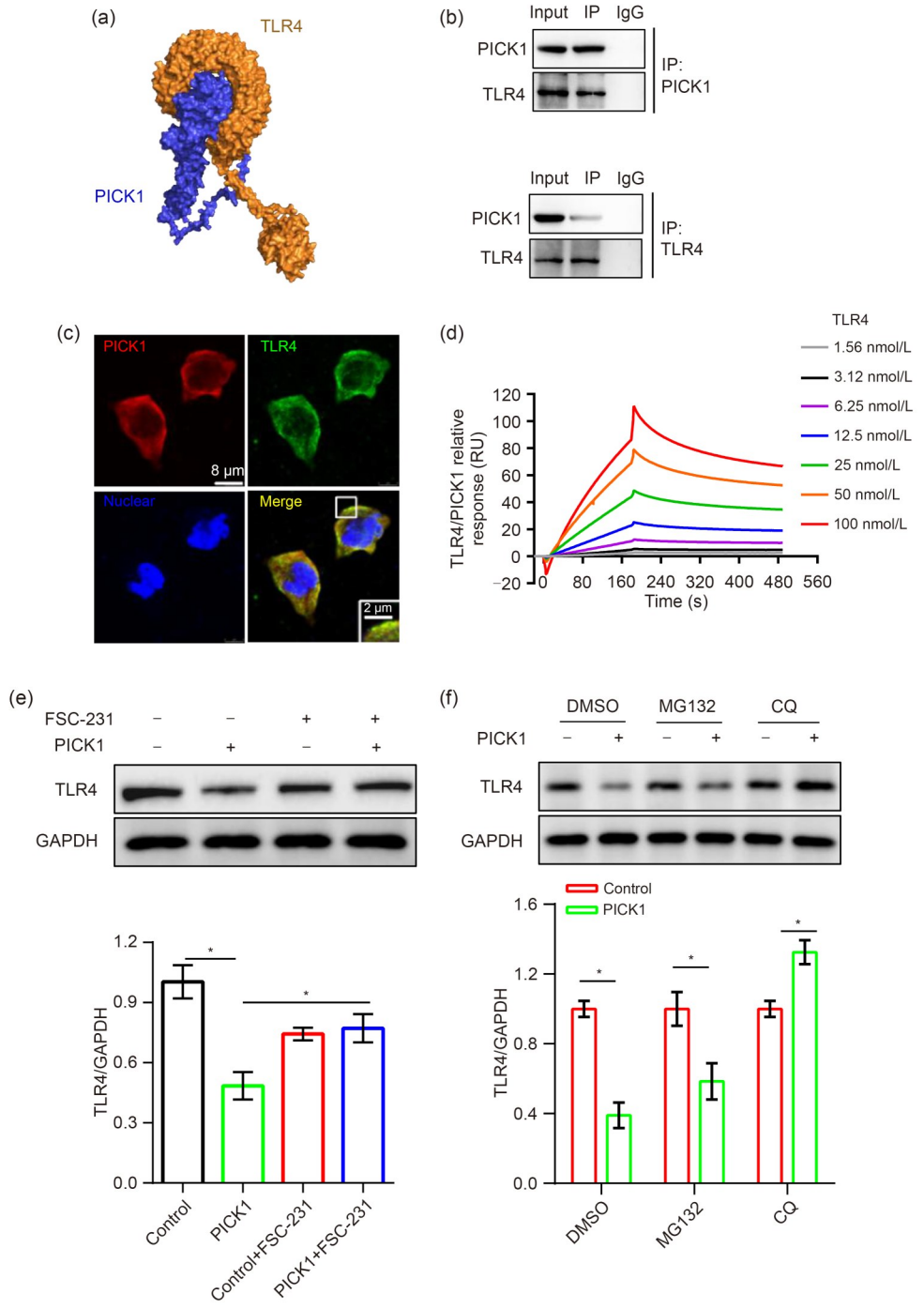

Fig. 5 Interaction between PICK1 and TLR4. (a) 3D structure of PICK1 with TLR4. (b) PICK1 and TLR4 levels in HEK293T cell lysates were measured using western blotting after IP with mouse anti-PICK1 or rabbit anti-TLR4. (c) PICK1 and TLR4 were colocalized in the HEK293T cells, as demonstrated by immunofluorescence. (d) Direct interaction between PICK1 and TLR4 was confirmed using SPR analysis. (e) The protein expression level of TLR4 was detected with or without FSC-231 stimulation by western blotting. (f) Cells were preincubated with DMSO, MG132, and CQ, and the expression of TLR4 was assessed by western blotting. The data are presented as mean±SD, $n \geq 3$. $^{*}P<0.05$. SD: standard deviation; PICK1: protein interacting with C kinase 1; TLR4: Toll-like receptor 4; GAPDH: glyceraldehyde-3-phosphate dehydrogenase; SPR: surface plasmon resonance; IP: immunoprecipitation; IgG: immunoglobulin G; DMSO: dimethyl sulfoxide; CQ: chloroquine.

Table 2 Binding energies of PICK1 and TLR4

Energy	0 ns			50 ns		
	Average (kcal/mol)	SD (kcal/mol)	SEM (kcal/mol)	Average (kcal/mol)	SD (kcal/mol)	SEM (kcal/mol)
ΔE_{vdW}	−173.6700	14.8953	1.0207	−209.1995	10.7279	2.2369
ΔE_{elec}	−62.4061	7.7085	5.7776	−86.1578	8.6800	8.0653
ΔE_{GB}	138.3554	16.3787	5.5003	132.3733	13.3863	6.3360
ΔE_{surf}	−24.6977	1.6405	0.1336	−34.2337	1.7317	0.1526
ΔG_{gas}	−236.0761	18.6261	5.9690	−295.3573	14.4785	7.1893
ΔG_{solv}	113.6577	26.2400	5.4714	98.1396	3.3708	6.3327
ΔG_{bind}	−122.4184	7.0067	1.4610	−197.2176	11.3316	2.3628

SD: standard deviation; SEM: standard error of the mean; ΔE_{vdW}: van der Waals energy; ΔE_{elec}: electrostatic energy; ΔE_{GB}: polar solvation-free energy; ΔE_{surf}: nonpolar solvation-free energy; ΔG_{gas}: gas-phase energy; ΔG_{solv}: solvation-free energy; ΔG_{bind}: binding-free energy.

(Figs. 6e and 6f). The details of the binding amino acid pairs are shown in Table S6. The ΔG_{bind} changed from −122.42 to −197.22 kcal/mol in the MD simulations. The interaction of the protein PICK1 with TLR4 was promoted by ΔE_{vdW} and ΔE_{elec}, and ΔE_{GB} and ΔG_{solv} generated energy losses in overcoming desolvation (Table 2). These results revealed the relative stability of the PICK1-TLR4 complex. The interaction network between them was gradually optimized during MD simulations, and this network is crucial for maintaining the mechanical properties of PICK1.

4 Discussion

PICK1, widely expressed in various tissues, is involved in the transport of membrane receptors through a single PDZ domain (Ramsakha et al., 2023). Abnormal PICK1 expression has been associated with invasion and metastasis in some tumors, including gastric cancer (Zhang et al., 2010; Dai et al., 2017). In this study, PICK1 expression was found to be decreased in human gastric tissues, which was predictive of poorer outcomes in patients. PICK1 overexpression suppressed gastric cell growth and migration and caused cell cycle arrest at the G_0/G_1 phase. Mechanistically, we demonstrated that PICK1 directly binds to TLR4, thereby promoting TLR4 degradation and decreasing inflammation-related protein levels (Fig. 3). We also observed a complex interaction network at the binding interface between PICK1 and TLR4. Our results indicate that PICK1 is associated with the regulation of cell metastasis and inflammation and may be a useful therapeutic target for the treatment of human gastric cancer.

Inflammation has been linked to the activation of EMT in many cancers (Ebrahimi et al., 2022). Changes in the inflammatory environment have been identified as key avenues for the treatment of human cancers. TLR4, an important molecule in inflammation-associated carcinogenesis, is a type I transmembrane protein that consists of three distinct structural domains: a leucine-rich repeat-containing ectodomain involved in pathogen-specific ligand recognition, a transmembrane domain, and a cytosolic domain that binds downstream adaptor proteins (Fukata and Abreu, 2008; Yuan et al., 2013). Studies have demonstrated that gastric cancer cell lines and cells express high levels of TLR4, which correlate with tumor stage and patient survival (Fernandez-Garcia et al., 2014; Taguchi and Mukai, 2019). Our research indicated that TLR4 expression was downregulated in PICK1-overexpressing human gastric cancer cells.

However, FSC-231 pretreatment significantly upregulated TLR4 expression in PICK1-overexpressing cells. TLR4 is located mainly in the endoplasmic reticulum (ER) and Golgi apparatus of quiescent cells. LPS stimulation causes the rapid migration of TLR4 from the Golgi apparatus to the cell membrane (Rocuts et al., 2010). However, recent evidence suggests that PICK1 plays an important role in the transport of various vesicles from the Golgi complex to several cellular systems, including neurons (Xu et al., 2016). PICK1 also interacts with Golgi-related PDZ and may be involved in vesicular transport from the Golgi apparatus to the acrosome (Xiao et al., 2009). Colocalization analysis by immunofluorescence revealed that TLR4 resides mainly in the cytoplasm when present in PICK1-overexpressing cells. PICK1 and TLR4 interact with each other via co-immunoprecipitation and

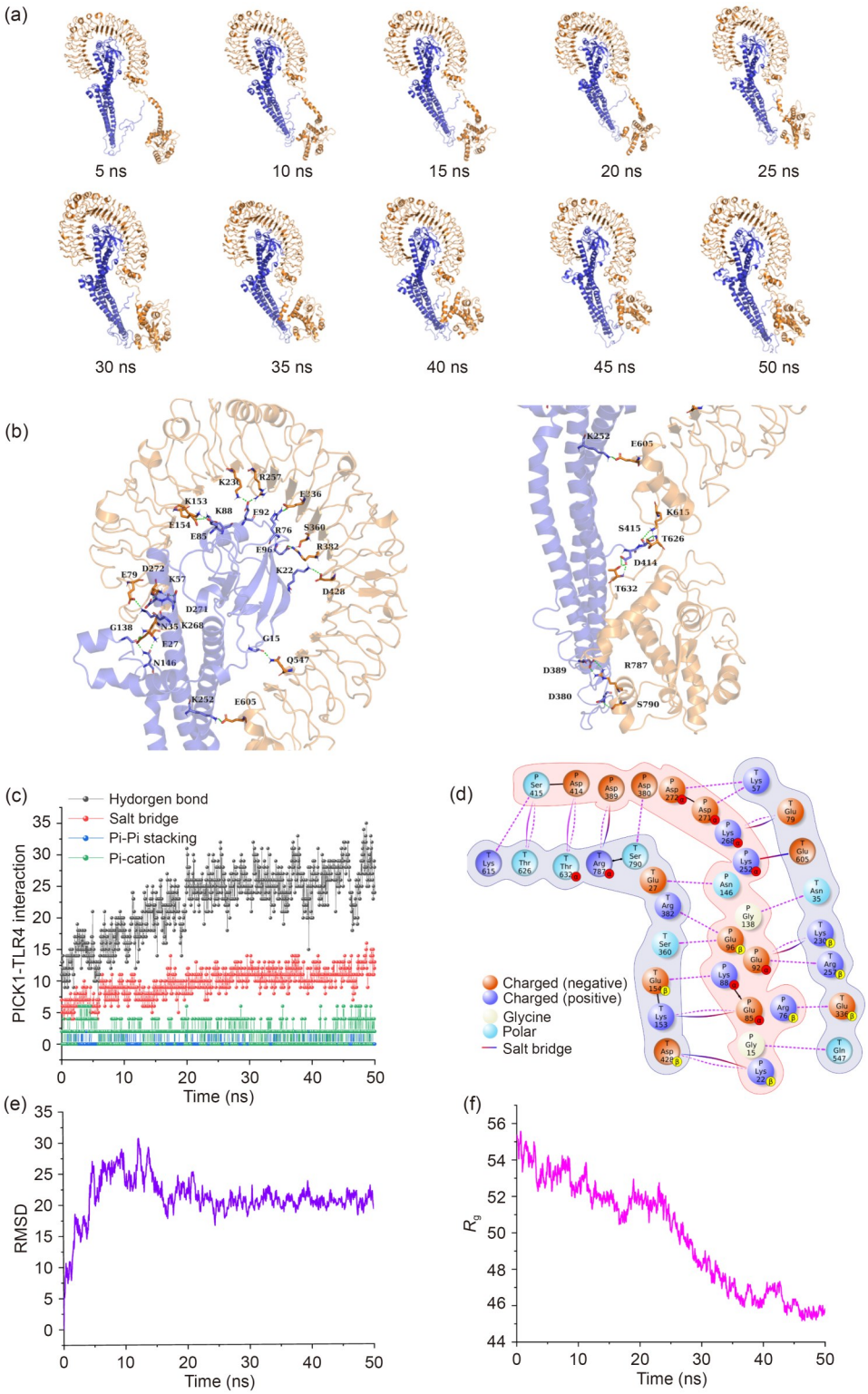

Fig. 6 Binding energy of PICK1 and TLR4 according to molecular dynamics simulations. (a) Structural characteristics of the complexes in 50 ns. (b) 3D structures. The hydrogen bond is represented by dotted green lines. (c) Molecular interatomic forces in the PICK1-TLR4 complex. (d) 2D structures. The hydrogen bond is represented by dotted lines; the salt bridge is represented by colored lines. (e, f) RMSD and R_g analyses. PICK1: protein interacting with C kinase 1; TLR4: Toll-like receptor 4; RMSD: root-mean-square deviation; R_g: radius of gyration.

SPR. Autophagic inhibitors significantly suppressed PICK1-induced TLR4 downregulation (Fig. 5). Our study suggests that PICK1 overexpression may alter the trafficking of TLR4 and enhance TLR4 degradation via autophagosomes. However, the specific degradation process is not yet clear and should be further explored in future research.

Further experiments explored the effects of PICK1 on TLR4 and the interaction network between the TLR4-PICK1 complex. It is known that clustering and synaptic targeting of PICK1 are dependent on the PDZ domain-mediated direct interaction at lipid membranes (Pan et al., 2007). The PDZ domain binds to the Eph receptor tyrosine kinase family and its ephrin ligands, affecting the oncogenesis and migration of tumor cells (Torres et al., 1998; Son et al., 2014; Liu et al., 2019). We also observed that PDZ domain inhibitors significantly suppressed PICK1-induced TLR4. We further determined the binding energies of PICK1 and TLR4 using MD simulations, and the data showed that interactions in the complex were reflected mainly by hydrogen bonds and salt-bridge bonding (Fig. 6).

In summary, this study demonstrated that PICK1 modulates TLR4-mediated metastasis and inflammation in gastric cells, providing novel insights into the progression and treatment of human gastric cancer and supplying additional information for a better understanding of PICK1 cellular and pathological functions.

5 Conclusions

In summary, our study demonstrated that high expression of PICK1 inhibited the malignant progression of gastric cancer. PICK1 inhibited gastric cancer cell proliferation and migration in vitro, which is dependent on the TLR4/MyD88 signaling pathway. These results provide new insights into gastric cancer treatment.

Data availability statement

The data presented in this study are available from the corresponding author upon reasonable request.

Acknowledgments

This work was supported by the National Natural Science Foundation of China (No. 82172363), the Traditional Chinese Medicine Scientific Research Project of Zhejiang Province (No. 2023ZL010), and the Zhejiang Medical and Health Science and Technology Project (Nos. 2022KY529 and 2024KY636), China. We thank Editage (https://www.editage.cn) for English language editing.

Author contributions

Kaiqiang LI, Yimin YANG, and Yaling WANG contributed equally to conceptualization, methodology, formal analysis, data curation, and writing – original draft. Jing JIN, Qianni WANG, and Lina PENG contributed to sample collection, data curation, and supervision. Aibo XU and Xuling LUO contributed to data curation and visualization. Wei YANG and Peng XU contributed to investigation and writing – review & editing. Bingyu CHEN, Ke HAO, and Zhen WANG contributed to funding acquisition and project administration. All authors have read and approved the final manuscript, and therefore, have full access to all the data in the study and take responsibility for the integrity and security of the data.

Compliance with ethics guidelines

Kaiqiang LI, Yimin YANG, Yaling WANG, Jing JIN, Qianni Wang, Lina PENG, Aibo XU, Xuling LUO, Wei YANG, Peng XU, Bingyu CHEN, Ke HAO, and Zhen WANG declare that they have no conflicts of interest.

The clinical specimens were obtained from Zhejiang Provincial People's Hospital and the National Human Genetic Resources Sharing Service Platform. The protocol was approved by the Ethics Committee of the Zhejiang Provincial People's Hospital (No. 2020QT312) and Shanghai Outdo Biotech Co., Ltd. (No. SHYJS-CP-1801015/YBM-05-02). The study was conducted in accordance with the guidelines of the Declaration of Helsinki.

References

Baron A, Deval E, Salinas M, et al., 2002. Protein kinase C stimulates the acid-sensing ion channel ASIC2a via the PDZ domain-containing protein PICK1. *J Biol Chem*, 277(52):50463-50468. https://doi.org/10.1074/jbc.M208848200

Batista TP, de Araújo Lima Santos CA, Almeida GFG, 2013. Perioperative chemotherapy in locally advanced gastric cancer. *Arq Gastroenterol*, 50(3):236-242. https://doi.org/10.1590/S0004-28032013000200042

Bedart C, Renault N, Chavatte P, et al., 2022. SINAPs: a software tool for analysis and visualization of interaction networks of molecular dynamics simulations. *J Chem Inf Model*, 62(6):1425-1436. https://doi.org/10.1021/acs.jcim.1c00854

Chen R, Alvero AB, Silasi DA, et al., 2008. Cancers take their Toll—the function and regulation of Toll-like receptors in cancer cells. *Oncogene*, 27(2):225-233. https://doi.org/10.1038/sj.onc.1210907

Chen XJ, Zhao F, Zhang HH, et al., 2015. Significance of TLR4/MyD88 expression in breast cancer. *Int J Clin Exp Pathol*, 8(6):7034-7039.

Cockbill LMR, Murk K, Love S, et al., 2015. Protein interacting with C kinase 1 suppresses invasion and anchorage-independent growth of astrocytic tumor cells. *Mol Biol Cell*, 26(25):4552-4561. https://doi.org/10.1091/mbc.E15-05-0270

Dai YH, Ren D, Yang Q, et al., 2017. The TGF-β signalling negative regulator PICK1 represses prostate cancer metastasis to bone. *Br J Cancer*, 117(5):685-694. https://doi.org/10.1038/bjc.2017.212

Ebrahimi N, Adelian S, Shakerian S, et al., 2022. Crosstalk between ferroptosis and the epithelial-mesenchymal transition: implications for inflammation and cancer therapy. *Cytokine Growth Factor Rev*, 64:33-45. https://doi.org/10.1016/j.cytogfr.2022.01.006

Fernandez-Garcia B, Eiró N, González-Reyes S, et al., 2014. Clinical significance of Toll-like receptor 3, 4, and 9 in gastric cancer. *J Immunother*, 37(2):77-83. https://doi.org/10.1097/CJI.0000000000000016

Fukata M, Abreu MT, 2008. Role of Toll-like receptors in gastrointestinal malignancies. *Oncogene*, 27(2):234-243. https://doi.org/10.1038/sj.onc.1210908

Gainetdinov RR, Caron MG, 2003. Monoamine transporters: from genes to behavior. *Annu Rev Pharmacol Toxicol*, 43:261-284. https://doi.org/10.1146/annurev.pharmtox.43.050802.112309

Giros B, Jaber M, Jones SR, et al., 1996. Hyperlocomotion and indifference to cocaine and amphetamine in mice lacking the dopamine transporter. *Nature*, 379(6566):606-612. https://doi.org/10.1038/379606a0

Hanley JG, 2008. PICK1: a multi-talented modulator of AMPA receptor trafficking. *Pharmacol Ther*, 118(1):152-160. https://doi.org/10.1016/j.pharmthera.2008.02.002

Hanley JG, Henley JM, 2005. PICK1 is a calcium-sensor for NMDA-induced AMPA receptor trafficking. *EMBO J*, 24(18):3266-3278. https://doi.org/10.1038/sj.emboj.7600801

Inoue K, 2007. UDP facilitates microglial phagocytosis through P2Y6 receptors. *Cell Adh Migr*, 1(3):131-132. https://doi.org/10.4161/cam.1.3.4937

Jaulin-Bastard F, Saito H, le Bivic A, et al., 2001. The ERBB2/HER2 receptor differentially interacts with ERBIN and PICK1 PSD-95/DLG/ZO-1 domain proteins. *J Biol Chem*, 276(18):15256-15263. https://doi.org/10.1074/jbc.M010032200

Jones SR, Gainetdinov RR, Jaber M, et al., 1998. Profound neuronal plasticity in response to inactivation of the dopamine transporter. *Proc Natl Acad Sci USA*, 95(7):4029-4034. https://doi.org/10.1073/pnas.95.7.4029

Lee KW, Park SR, Oh DY, et al., 2013. Phase I study of sunitinib plus capecitabine/cisplatin or capecitabine/oxaliplatin in advanced gastric cancer. *Invest New Drugs*, 31(6):1547-1558. https://doi.org/10.1007/s10637-013-0032-y

Liu R, Yu RZ, Cui YX, et al., 2019. Inhibitory effect of taspine derivative TAD1822-7 on tumor cell growth and angiogenesis *via* suppression of EphrinB2 and related signaling pathways. *Acta Pharm*, 69(3):423-431. https://doi.org/10.2478/acph-2019-0021

Lorgen JØ, Egbenya DL, Hammer J, et al., 2017. PICK1 facilitates lasting reduction in GluA2 concentration in the hippocampus during chronic epilepsy. *Epilepsy Res*, 137:25-32. https://doi.org/10.1016/j.eplepsyres.2017.08.012

Lu W, Ziff EB, 2005. PICK1 interacts with ABP/GRIP to regulate AMPA receptor trafficking. *Neuron*, 47(3):407-421. https://doi.org/10.1016/j.neuron.2005.07.006

Meliț LE, Mărginean CO, Mărginean CD, et al., 2019. The relationship between toll-like receptors and *Helicobacter pylori*-related gastropathies: still a controversial topic. *J Immunol Res*, 2019:8197048. https://doi.org/10.1155/2019/8197048

Mohammadi E, Joshi SY, Deshmukh SA, 2023. Development, validation, and applications of nonbonded interaction parameters between coarse-grained amino acid and water models. *Biomacromolecules*, 24(9):4078-4092. https://doi.org/10.1021/acs.biomac.3c00441

Pan LF, Wu H, Shen C, et al., 2007. Clustering and synaptic targeting of PICK1 requires direct interaction between the PDZ domain and lipid membranes. *EMBO J*, 26(21):4576-4587. https://doi.org/10.1038/sj.emboj.7601860

Park SC, Chun HJ, 2013. Chemotherapy for advanced gastric cancer: review and update of current practices. *Gut Liver*, 7(4):385-395. https://doi.org/10.5009/gnl.2013.7.4.385

Pasare C, Medzhitov R, 2005. Toll-like receptors: linking innate and adaptive immunity. *In*: Gupta S, Paul WE, Steinman R (Eds.), Mechanisms of Lymphocyte Activation and Immune Regulation X. Springer, Boston, p.11-18. https://doi.org/10.1007/0-387-24180-9_2

Rakoff-Nahoum S, Medzhitov R, 2009. Toll-like receptors and cancer. *Nat Rev Cancer*, 9(1):57-63. https://doi.org/10.1038/nrc2541

Ramsakha N, Ojha P, Pal S, et al., 2023. A vital role for PICK1 in the differential regulation of metabotropic glutamate receptor internalization and synaptic AMPA receptor endocytosis. *J Biol Chem*, 299(6):104837. https://doi.org/10.1016/j.jbc.2023.104837

Rocca DL, Martin S, Jenkins EL, et al., 2008. Inhibition of Arp2/3-mediated actin polymerization by PICK1 regulates neuronal morphology and AMPA receptor endocytosis. *Nat Cell Biol*, 10(3):259-271. https://doi.org/10.1038/ncb1688

Rocuts F, Ma YH, Zhang XY, et al., 2010. Carbon monoxide suppresses membrane expression of TLR4 via myeloid differentiation factor-2 in βTC3 cells. *J Immunol*, 185(4):2134-2139. https://doi.org/10.4049/jimmunol.0902782

Shoaib TH, Almogaddam MA, Andijani YS, et al., 2023. Marine-derived compounds for CDK5 inhibition in cancer: integrating multi-stage virtual screening, MM/GBSA

analysis and molecular dynamics investigations. *Metabolites*, 13(10):1090. https://doi.org/10.3390/metabo13101090

Siegel RL, Miller KD, Wagle NS, et al., 2023. Cancer statistics, 2023. *CA Cancer J Clin*, 73(1):17-48. https://doi.org/10.3322/caac.21763

Son J, Park MS, Park I, et al., 2014. Pick1 modulates ephrinB1-induced junctional disassembly through an association with ephrinB1. *Biochem Biophys Res Commun*, 450(1):659-665. https://doi.org/10.1016/j.bbrc.2014.06.027

Stein A, Arnold D, Thuss-Patience PC, et al., 2014. Docetaxel, oxaliplatin and capecitabine (TEX regimen) in patients with metastatic gastric or gastro-esophageal cancer: results of a multicenter phase I/II study. *Acta Oncologica*, 53(3):392-398. https://doi.org/10.3109/0284186X.2013.833346

Taguchi T, Mukai K, 2019. Innate immunity signalling and membrane trafficking. *Curr Opin Cell Biol*, 59:1-7. https://doi.org/10.1016/j.ceb.2019.02.002

Torres GE, Yao WD, Mohn AR, et al., 2001. Functional interaction between monoamine plasma membrane transporters and the synaptic PDZ domain-containing protein PICK1. *Neuron*, 30(1):121-134. https://doi.org/10.1016/S0896-6273(01)00267-7

Torres R, Firestein BL, Dong HL, et al., 1998. PDZ proteins bind, cluster, and synaptically colocalize with Eph receptors and their ephrin ligands. *Neuron*, 21(6):1453-1463. https://doi.org/10.1016/S0896-6273(00)80663-7

Vani BP, Aranganathan A, Tiwary P, 2024. Exploring kinase Asp-Phe-Gly (DFG) loop conformational stability with AlphaFold2-RAVE. *J Chem Inf Model*, 64(7):2789-2797. https://doi.org/10.1021/acs.jcim.3c01436

Wang EL, Qian ZR, Nakasono M, et al., 2010. High expression of Toll-like receptor 4/myeloid differentiation factor 88 signals correlates with poor prognosis in colorectal cancer. *Br J Cancer*, 102(5):908-915. https://doi.org/10.1038/sj.bjc.6605558

Xia J, Zhang XQ, Staudinger J, et al., 1999. Clustering of AMPA receptors by the synaptic PDZ domain-containing protein PICK1. *Neuron*, 22(1):179-187. https://doi.org/10.1016/S0896-6273(00)80689-3

Xiao N, Kam C, Shen C, et al., 2009. PICK1 deficiency causes male infertility in mice by disrupting acrosome formation. *J Clin Invest*, 119(4):802-812. https://doi.org/10.1172/JCI36230

Xu JY, Wang N, Luo JH, et al., 2016. Syntabulin regulates the trafficking of PICK1-containing vesicles in neurons. *Sci Rep*, 6:20924. https://doi.org/10.1038/srep20924

Yan YM, Tao HY, He JH, et al., 2020. The HDOCK server for integrated protein–protein docking. *Nat Protoc*, 15(5):1829-1852. https://doi.org/10.1038/s41596-020-0312-x

Yang J, Liu DP, Khatri KS, et al., 2016. Prognostic value of toll-like receptor 4 and nuclear factor-κBp65 in oral squamous cell carcinoma patients. *Oral Surg Oral Med Oral Pathol Oral Radiol*, 122(6):753-764.e1. https://doi.org/10.1016/j.oooo.2016.08.002

Yuan X, Zhou Y, Wang W, et al., 2013. Activation of TLR4 signaling promotes gastric cancer progression by inducing mitochondrial ROS production. *Cell Death Dis*, 4(9):e794. https://doi.org/10.1038/cddis.2013.334

Zhang B, Cao WF, Zhang F, et al., 2010. Protein interacting with C α kinase 1 (PICK1) is involved in promoting tumor growth and correlates with poor prognosis of human breast cancer. *Cancer Sci*, 101(6):1536-1542. https://doi.org/10.1111/j.1349-7006.2010.01566.x

Zhang HJ, Zhang SL, 2017. The expression of Foxp3 and TLR4 in cervical cancer: association with immune escape and clinical pathology. *Arch Gynecol Obstet*, 295(3):705-712. https://doi.org/10.1007/s00404-016-4277-5

Zhou Y, Li KQ, Du YQ, et al., 2021. Protein interacting with C-kinase 1 is involved in epithelial-mesenchymal transformation and suppresses progress of gastric cancer. *Med Oncol*, 38(4):34. https://doi.org/10.1007/s12032-021-01483-0

Supplementary information

Tables S1–S6; Figs. S1–S4